Received: 27 June 2018 | Revised: 10 September 2018 | Accepted: 24 September 2018

DOI: 10.1111/epi.14583

FULL-LENGTH ORIGINAL RESEARCH

Epilepsia®

Subcentimeter epilepsy surgery targets by resting state functional magnetic resonance imaging can improve outcomes in hypothalamic hamartoma

Varina L. Boerwinkle[1] | Stephen T. Foldes[2] | Salvatore J. Torrisi[3] | Hamy Temkit[4] | William D. Gaillard[5] | John F. Kerrigan[1] | Virendra R. Desai[6] | Jeffrey S. Raskin[7] | Aditya Vedantam[7] | Randa Jarrar[1] | Korwyn Williams[1] | Sandi Lam[7] | Manish Ranjan[8] | Janna S. Broderson[9] | David Adelson[1,8] | Angus A. Wilfong[1] | Daniel J. Curry[7]

[1]Division of Pediatric Neurology, Barrow Neurological Institute at Phoenix Children's Hospital, Phoenix, Arizona

[2]Neuroscience Research, Barrow Neurological Institute at Phoenix Children's Hospital, Phoenix, Arizona

[3]Section on the Neurobiology of Fear and Anxiety, National Institute of Mental Health, National Institutes of Health, Bethesda, Maryland

[4]Department of Research, Phoenix Children's Hospital, Phoenix, Arizona

[5]Department of Neurology, Children's National Medical Center, Washington, District of Columbia

[6]Department of Neurosurgery, Houston Methodist Hospital, Houston Methodist Neurological Institute, Houston, Texas

[7]Department of Pediatric Neurosurgery, Texas Children's Hospital, Baylor College of Medicine, Houston, Texas

[8]Division of Pediatric Neurosurgery, Barrow Neurological Institute at Phoenix Children's Hospital, Phoenix, Arizona

[9]Division of Pediatric Neurology, Texas Children's Hospital, Baylor College of Medicine, Houston, Texas

Correspondence
Varina L. Boerwinkle, Division of Pediatric Neurology, Barrow Neurological Institute at Phoenix Children's Hospital,

Summary

Objective: The purpose of this study is to investigate the outcomes of epilepsy surgery targeting the subcentimeter-sized resting state functional magnetic resonance imaging (rs-fMRI) epileptogenic onset zone (EZ) in hypothalamic hamartoma (HH).

Methods: Fifty-one children with HH-related intractable epilepsy received anatomical MRI-guided stereotactic laser ablation (SLA) procedures. Fifteen of these children were control subjects (CS) not guided by rs-fMRI. Thirty-six had been preoperatively guided by rs-fMRI (RS) to determine EZs, which were subsequently targeted by SLA. The primary outcome measure for the study was a predetermined goal of 30% reduction in seizure frequency and improvement in class I Engel outcomes 1 year postoperatively. Quantitative and qualitative volumetric analyses of total HH and ablated tissue were also assessed.

Results: In the RS group, the EZ target within the HH was ablated with high accuracy (>87.5% of target ablated in 83% of subjects). There was no difference between the groups in percentage of ablated hamartoma volume ($P = 0.137$). Overall seizure reduction was higher in the rs-fMRI group: 85% RS versus 49% CS ($P = 0.0006$, adjusted). The Engel Epilepsy Surgery Outcome Scale demonstrated significant differences in those with freedom from disabling seizures (class I), 92% RS versus 47% CS, a 45% improvement ($P = 0.001$). Compared to prior studies, there was improvement in class I outcomes (92% vs 76%-81%). No postoperative morbidity or mortality occurred.

Significance: For the first time, surgical SLA targeting of subcentimeter-sized EZs, located by rs-fMRI, guided surgery for intractable epilepsy. Our outcomes demonstrated the highest seizure freedom rate without surgical complications and are a significant improvement over prior reports. The approach improved freedom

Phoenix, AZ 85016.
Email: vboerwinkle@phoenixchildrens.com

Funding information
Varina Boerwinkle received a grant from Hope for Hypothalamic Hamartomas to analyze and publish the results of the work performed for this article.

from seizures by 45% compared to conventional ablation, regardless of hamartoma size or anatomical classification. This technique showed the same or reduced morbidity (0%) compared to recent non–rs-fMRI-guided SLA studies with as high as 20% permanent significant morbidity.

KEYWORDS
epilepsy surgery, functional connectivity, hypothalamic hamartoma, intractable epilepsy, resting state functional MRI

1 | INTRODUCTION

Over the past 30 years, innovations in medications have not improved the cure rate of focal epilepsy.[1] However, some focal epilepsies are the result of structural abnormalities in the brain that can be imaged and targeted for intervention. Surgical intervention offers a potential cure for these focal epilepsies by destroying the epileptogenic zone (EZ). The EZ is an "area of brain that is necessary and sufficient for initiating seizures and whose removal (or disconnection) is necessary for complete abolition of seizures."[2] Localizing the EZ to a small, subcentimeter area also reduces the surgical target size. This allows for less invasive solutions and decreased surgical morbidity, while maintaining or improving seizure outcomes. Correctly localizing and targeting a small EZ is a critical goal in epilepsy treatment.

One epilepsy population in whom EZ localization has been shown to be impervious to current noninvasive technologies are those individuals with a hypothalamic hamartoma (HH).[3–5] Hamartomas can range in size from 2 to 30 mm^3.[6] Furthermore, the location of an EZ inside an HH appears to be relatively random, as shown from in vivo depth electrode and postmortem stromal evidence.[6]

In trying to understand what pattern can be determined regarding HH EZ anatomy, consideration should be given to the finding that some HHs are not associated with seizures and are primarily discovered from endocrinologically based dysfunction at presentation. Those HHs that do cause seizures are brought to a clinician's attention typically due to gelastic or laughter-associated seizures.[5] Thus, some HHs are connected to the rest of the brain in a way that produces seizures, whereas others apparently have no such epilepsy-inducing connection. The HH is a different structure from the hypothalamus itself; it consists of ectopic tissue containing clusters of connected and unconnected neurons.[7,8] The way in which an HH connects to the hypothalamus, a small, centralized, and evolutionarily conserved structure with many subregions, is critical to the resulting HH presentation and phenotype.

The hypothalamus has well-established connections to the rest of the brain through the mammillothalamic tract and the fornix.[9] The smaller fibers from the hypothalamus run through the ventral septum and nucleus retroambiguus within the pons.[10] The HH ictal propagation pathway starts with seizures generated in the HH, then spreads to downstream areas such as the anterior thalamus, hippocampus, occipitotemporal junction, and other specific areas.[11–14] This has been studied with electroencephalographic functional magnetic resonance imaging (fMRI),[11,13] intracranial electroencephalography,[14] and ictal single photon emission computed tomography.[12] The areas found to have the highest ictal epileptogenic spread are via these hypothalamic white matter tracts.

Key Points

- For the first time, surgical SLA targeting of subcentimeter-sized EZs, located by rs-fMRI, guided surgery for an intractable epilepsy
- The approach improved freedom from seizures by 45% compared to conventional ablation, regardless of hamartoma size
- This technique showed the same or reduced morbidity (0%) compared to other recent studies with as high as 20% permanent significant morbidity

Resting state fMRI (rs-fMRI) is an established, in vivo, and noninvasive method to elucidate functional brain connectivity of both cortical and subcortical structures.[15] To determine whether rs-fMRI can be relied upon to localize EZ in an HH, it is important to know whether rs-fMRI can replicate these previous ictal-spread studies. Our group has previously shown that areas of ictal propagation can be localized using rs-fMRI.[16] Furthermore, that study showed that rs-fMRI was able to differentiate areas of initial seizure propagation from those of downstream epileptogenic spread. Thus, rs-fMRI is a plausible solution, with no requirement of an a priori EZ location hypothesis, to advance treatment and postsurgical safety profile in the HH epilepsy population.

Regarding this safety profile, traditional invasive surgical methods have notable morbidity and mortality in this population, with frequent postsurgical endocrinological

disorders (diabetes insipidus, hypothyroidism, and growth hormone deficiency), catastrophic intellectual memory loss, new or worsened emotional dysregulation,[5,17,18] and death reported as high as 10%.[19]

In HH, modern and less-invasive surgical methods, such as stereotactic laser ablation (SLA), have improved surgical morbidity, mortality, and seizure freedom ranging from 66% to 81%.[5,20–22] Despite this improvement, there remains significant and permanent morbidity in postsurgical HH cases reportedly as high as 20%.[22] This may be due to a proposed need to disconnect the HH from the rest of the brain at the HH border zone.[23] The HH border zone, however, contains critical structures necessary for memory (fornix and mammillary bodies), endocrine function (hypothalamus), and motor control (internal capsule).[5,24] By being able to localize the EZ deeper inside the HH, at increased distance from these critical structures, the surgeon may destroy or disconnect this tissue with better outcome.

rs-fMRI also has precedent in localizing neurological diseases as focal disruptions in the blood oxygenation level–dependent signal.[15] rs-fMRI is one proposed noninvasive method of localizing EZ that is additionally capable of probing deep, subcortical structures.[3,25,26] For the sake of terminological simplicity, the term "EZ" is used here to mean the area identified by rs-fMRI and subsequently targeted by SLA. With the exception of one case report,[27] these prior rs-fMRI studies' EZs were larger than subcentimeter. Due to the standard limitation of the SLA ablation target size being 2 cm in diameter, EZs beyond this size threshold are less helpful as surgical targets, especially if the true seizure onset zone is smaller.

In the present study, preoperative rs-fMRI was used in a pediatric HH population with intractable epilepsy to independently locate subcentimeter-sized EZs within the HH. SLA was then used to directly target the proposed EZ, and the seizure and morbidity outcomes were observed. It was hypothesized that targeted ablation of the EZ would reduce seizure burden by at least 30% compared to those with SLA not guided by rs-fMRI EZ. This seemed a reasonable goal to make surgery worthwhile, increase the number of Engel I category responders,[28] and reduce surgical morbidity.

2 | MATERIALS AND METHODS

The main advancement of this technique is developing and applying a novelty combined rs-fMRI analysis method. This two-step method would allow the larger abnormal area, identified by independent component analysis (ICA), to be parsed to a subcentimeter zone, hypothesized to be critical for ablation to abolish seizures.

First, a well-established, data-driven processes of ICA was used to remove nonneuronal, scanner artifact, and physiological noise signals from the rs-fMRI data.[29,30] We have previously published on the use of ICA in pediatric epilepsy to distinguish noise from EZs, which had 90% correlation with postsurgical outcomes.[3]

Second, the denoised rs-fMRI was used to examine every voxel of the HH and its connectivity to the rest of the brain. Pearson correlations were calculated as measures of functional connectivity, which often also reflect direct structural connections between two regions.[31,32] If the HH voxel was determined to possess highly significant functional connectivity to areas of brain outside the HH, it was considered to be an EZ (see below for further details).

2.1 | Experimental design

The population studied was a consecutive series of pediatric patients with intractable epilepsy due to HH (Table 1). A total of 51 SLAs were performed on children with HH at Texas Children's Hospital from December 2012 to July 2016. Of these, 36 had a prospective rs-fMRI performed that was used to inform the laser targeting of the HH (RS group). The rs-fMRI scan was added to a standard clinical MRI battery with approval by the local institutional review board (IRB; H-32492) and obtained according to the Declaration of Helsinki.

The treating epilepsy team opted to offer rs-fMRI to all patients, given the preliminary data showing rs-fMRI EZ improved surgical outcomes with a good safety profile in the pediatric general epilepsy population.[3] The IRB determined that additional consent procedures were unnecessary because the rs-fMRIs were collected as part of a standard preoperative MRI. Although specific consent for the rs-fMRI sequence was not obtained in this cohort, all patient families were given the option to have an rs-fMRI and were aware that the patient underwent an additional rs-fMRI scan. Families were also aware rs-fMRI results would be reviewed by the epilepsy surgical planning team, may modify surgical planning, and would be explained to the family prior to surgery. If they did not have rs-fMRI, then standard planning of surgical targeting would occur.

Prior HH surgery methods were not guided by EZ. Instead, they used general anatomical targets, such as the border zone between the HH and the hypothalamus or the side of the HH with greater tissue mass. The neurosurgeon continued to take safety-related anatomical considerations into account, such as proximity to critical structures, while aiming the laser at the EZ. Thus, the clinicians and IRB committee determined the study plan's use of rs-fMRI introduced no increased risk over prior SLA therapy.

Patients were allocated to the control subject (CS) or rs-fMRI group (RS) based on the success of the rs-fMRI data acquisition (further details of the image acquisition, MRI sequence parameters, image preprocessing, surgical methods, and independent component [IC] thresholding are in Appendix S1). Adequate rs-fMRI failed in the CS for

TABLE 1 Demographics, seizure frequency, and hamartoma characteristics

	C, n = 15	RS, n = 36	Total, N = 51	*P*
Gender				0.5034[a]
F	3 (20.0%)	12 (33.3%)	15 (29.4%)	
M	12 (80.0%)	24 (66.7%)	36 (70.6%)	
Age, y				0.5696[b]
Mean (SD)	8.4 (5.3)	7.7 (5.4)	7.9 (5.4)	
Range	0.5-20.9	1.5-18.4	0.5-20.9	
Preoperative seizure frequency per week				0.1281[b]
Mean (SD)	65.9 (146.7)	83.1 (148.3)	78.0 (146.6)	
Range	2.0-588.0	1.5-756.0	1.5-756.0	
Hamartoma size, cm^3				0.7878[b]
Mean (SD)	7.0 (5.5)	8.6 (8.7)	8.1 (7.9)	
Range	1.6-23.5	0.9-28.3	0.9-28.3	
Delalande classification				0.1573[a]
1	2 (13.3%)	0 (0.0%)	2 (3.9%)	
2	8 (53.3%)	16 (44.4%)	24 (47.1%)	
3	2 (13.3%)	9 (25.0%)	11 (21.6%)	
4	3 (20.0%)	11 (30.6%)	14 (27.5%)	

Voxel size = 3.0 × 3.0 × 3.4 mm.
C, controls; F, female; M, male; RS, resting state group; SD, standard deviation.
[a]Fisher's exact.
[b]Wilcoxon rank-sum.

several reasons; the rs-fMRI was unintentionally not ordered or collected during scanning time (six patients), patient head motion was >1 mm in any direction causing loss of reliable signal and the introduction of artifacts (four patients), or there was lack of communication with the anesthesiologists to ensure a sufficiently low level of anesthetic (conscious sedation), resulting in suppression of rs-fMRI signal (five patients; see below for more details on sedation effects on rs-fMRI signal).

Demographics, seizure frequency, semiology, medication history, postoperative clinical course, and surgical outcomes were collected. Seizure frequency was recorded in family seizure diaries and reported to the treating epileptologist. Gelastic, partial, and generalized seizures were all considered for the seizure frequency analysis. Anatomical imaging using the preoperative MRI was utilized for determining HH laterality (right, left, bilateral), size, and any other cerebral anomalies, as determined by a radiologist.

2.2 | Surgical methods

All patients underwent SLA to their HH, and 48 of 51 procedures were performed with a single laser trajectory. In the RS group, the surgeon aimed the laser directly at the rs-fMRI EZ within the HH using MRI-guided intraoperative laser trajectory placement.

Stereotactic laser ablation involves drilling a 2-mm skull burr hole and inserting a 2-mm diameter tube from the top of the skull to the desired EZ target. The laser is passed through the tube to the EZ. The EZ tissue is exposed to the tip of the laser as it passes through the bottom end of the tube. The maximum laser target size is 20 mm in diameter. Thermal tissue destruction from the laser in HH is limited by the surrounding heat sink caused by cerebral fluid spaces (basal cisterns) and blood vessels.

In the control group, HH targeting was planned based on anatomy, as no prior technology noninvasively localizes EZ within the HH. Namely, if the HH appeared to have a more lateralized tissue bulk or anatomical connection thickness to one hemisphere, then that side of the HH was targeted. The targets in both groups had the same surgical safety considerations, including HH size and proximity to mammillary bodies, hypothalamus, fornix, and internal capsule.

2.3 | rs-fMRI analysis

rs-fMRI EZ targets were determined by a four-step process:

2.3.1 | Step 1: ICA

ICA was previously tested in a broader epilepsy surgery population and correlated with both intraoperative

electroencephalographic verification of rs-fMRI EZ localization and postoperative outcomes.[3]

When applying ICA to rs-fMRI signals, there are several oscillating signal sources per an individual's scan, called ICs. Most of these ICs are not signals of interest, as they are considered noise from nonneuronal sources.[30] Examples include noise generated by head motion, CSF pulsation, vascular pulsation, respiration, and scanners. The spatial and temporal patterns of the noise in our data have been published.[3] The IC classification paradigm is shown in Figure S1. Examples of IC are shown in Figure S2. Normal independent components of the brain are easily recognized for their slow oscillating time course and spatial distribution. Examples of normal neuronal networks are the "default mode," vision, language, and primary sensorymotor networks. At standard resting state scanning parameters, there are approximately 25 major normal large-scale brain networks in total, and these were detected in all patients. ICs were thresholded using the IC local false discovery rate for IC detection, set at $P < 0.05$.[33]

After visual classification, noise IC signals were regressed out of the rs-fMRI individual preprocessed blood oxygenation level–dependent signal. The percentage of ICs deemed noise was determined by the number of ICs in each subject's data meeting published noise spatial and temporal criteria.[3]

2.3.2 | Step 2: SearchLight

Following denoising, every voxel of the individual's HH was queried for functional connectivity via Pearson correlations through SearchLight (S.J.T. and V.L.B.). This in-house, automated version of AFNI's *InstaCorr*[34] queried the whole-brain functional connectivity of every individual HH voxel. SearchLight assigns each voxel a discrete coordinate and overlays it onto the preoperative, intraoperative, and remote postoperative images, creating multiple, concatenated images for manual evaluation (Figure 1). The SearchLight connectivity threshold was set uniformly at $r \leq -0.25$ and ≥ 0.25 for all patients. This threshold was previously found to detect significant connectivity between the HH and the initial area's seizure propagation reported by all other modalities.[17] The threshold was not varied to determine sensitivity to the final EZ size or shape, avoiding such subjectivity.

Images that showed connectivity between the HH and any portion of the rest of the brain were considered EZs, as any neurons within an HH are abnormal and should not be communicating outside of the HH. The preoperative images were prospectively rated by an expert neurologist (V.L.B.).

2.3.3 | Step 3: Verification of the accuracy of EZ surgical targeting

The preoperative connectivity EZ images were also overlaid on the immediate postoperative gradient echo, diffusion-weighted images and remote (>6 months from time of surgery) postoperative anatomic MRI images obtained 6 months to 1 year later (Figure S3). Two experienced neurosurgical fellows (J.S.R., V.R.D.) interpreted these images. The EZ was defined as being accurately targeted by the laser if the EZ was within an area of immediate postoperative diffusion restriction, contrast extravasation, or gliosis.

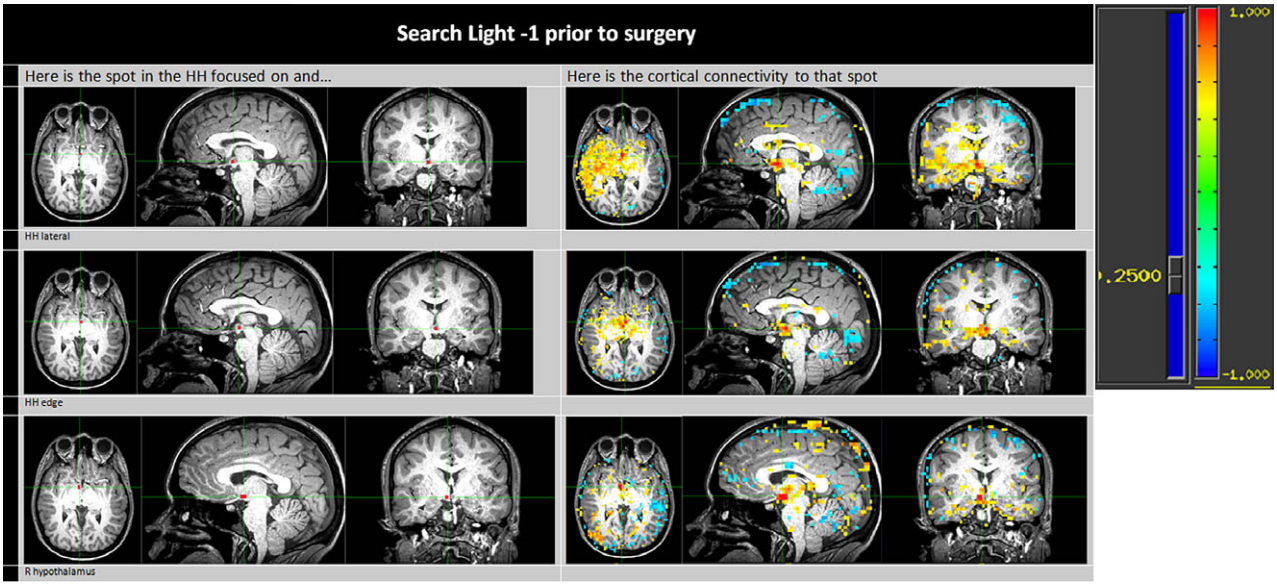

FIGURE 1 Examples of three hypothalamic hamartoma (HH) voxels (small red dots inside the HH) from a single patient are in the left column. The right column contains the connectivity from SearchLight to the voxel

If there was rater disagreement, a third reviewer broke the tie (V.L.B.). Lack of agreement between the two initial reviewers occurred in eight of 51 subjects. The agreement of the two primary raters on the voxel level across all subjects was 94% (95% confidence interval = 0.90%-0.97%), and consensus was obtained in all cases. The raters were blinded to the surgical seizure outcome and only given the images to determine whether the rs-fMRI target area was ablated.

2.3.4 | Step 4: Clinical correlation

Imaging results of the RS and CS groups were correlated with clinical outcomes of reduced seizure burden. Seizure burden included gelastic, generalized, focal, and absence seizures, as determined by the treating epileptologist 1 year postoperatively. Voxel locations and ablation status were digitized to analyze image statistics, as shown in Figure S4. Summary data included frequencies and proportions for categorical variables, mean and standard deviation, and median and range for continuous variables. Group comparisons were conducted using the Wilcoxon rank-sum test for continuous variables and the Fisher's exact test for categorical variables. The Pearson correlation coefficient was used to assess the linear association between continuous variables. Univariate and multiple regression analyses were conducted to model the percentage seizure reduction to provide adjusted comparisons between groups. The statistical results include regression parameter estimates, corresponding standard errors and 95% confidence intervals, and P values for statistical significance. The significance level was set at $P < 0.05$. Statistical analyses were performed using the statistical software packages SAS version 9.4 (SAS Institute, Cary, North Carolina) and R Studio version 1.0.153 (RStudio, Boston, Massachusetts).

3 | RESULTS

3.1 | Demographics and HH size comparison

There was no significant difference between the control and RS groups in gender, age, preoperative seizure frequency, total HH size, or Delalande anatomical classification (Table 1).[23] Delalande classifies HH according to midline, lateral, or intraventricular location, as well as whether it is giant in size.

3.2 | rs-fMRI EZ connectivity description results

The only ICs that remained after noise regression were those determined to be of neuronal origin. The total number of ICs per patient ranged from 56 to 144. The IC categorization and noise IC elimination algorithms were not altered to determine whether this changed the final EZ size or shape. Percentage of ICs deemed noise ranged from 50% to 68%, which is comparable to other investigators.[35]

All patients' rs-fMRI connectivity patterns from the ICA-SearchLight analysis demonstrated connectivity to the areas previously reported as the primary areas of ictal propagation.[16] These areas included the thalamus, anterior cingulate, hippocampus, occipitotemporal junction, parahippocampal gyrus, amygdala, anterior operculum, nucleus accumbens, and caudate.

3.3 | Surgical approach considering HH shape

Cylindrical anatomy is most ideal for SLA, allowing for ablation along a straight line of the laser trajectory. Therefore, the preoperative planning for those with HH tissue greater than the laser's thermal reach or noncylindrical anatomy necessitated leaving some residual, nonablated HH tissue postoperatively.

Thirty-one of 36 RS patients had hamartomas larger than the laser's effect size (10-20 mm diameter) or an anatomical configuration that was noncylindrical. Because there was no difference in HH volume or Delalande classification, there was also no appreciable difference in surgical planning complexity between groups.

Furthermore, given that only five RS patients had HHs smaller than the laser effect size, the impact of the rs-fMRI–derived EZ on surgical planning was high in most cases. The neurosurgeon planned the laser trajectory exactly at the EZ in all cases, with care to avoid all critical structures in the laser trajectory. In most cases, the trajectory was diagonal through the prefrontal cortex of the contralateral hemisphere and aimed toward the EZ. Care was taken to avoid internal capsule, mammillary bodies, mammillothalamic tract, and tissue immediately adjacent to the hypothalamus.

3.4 | Accuracy of EZ target ablation

The percentage in volume of hamartoma ablated did not differ between controls (50%) and RS (40%) patients ($P = 0.1366$; Table 2). However, the percentage of total EZ volume ablated was 87.5% or higher in 83% of subjects. The remainder had a range of 50%-80%. This indicates relatively high accuracy in targeting and ablation of the EZ, and avoidance of ablation of tissue outside the EZ. As the majority of EZs were nearly completely ablated, there were not enough patients with low EZ ablation to detect an association with the outcome. Further study is needed to make this determination.

The only tissue that received thermal laser ablation was within the boundaries of the hamartoma. Care was taken to

avoid ablating any other structures. The anatomical HH configuration (Delalande classification) and size were not found to be statistically different between the two groups. Therefore, the location of ablated hamartoma tissue, in relation to other brain structures, was not different between the two groups. This is illustrated in Figure S3, which shows an example RS EZ target voxel image from each patient overlaid on the postoperative ablation images.

3.5 | HH size and preoperative seizure frequency

After adjusting for group and presurgical seizure rate, the HH volume was inversely associated with the seizure outcome (beta coefficient = −0.053, $P = 0.007$). Presurgical seizure rates had no significant effect on surgical outcome ($P = 0.69$). See Table S2 for a summary.

3.6 | Primary outcome of seizure reduction

The primary aim was met of reducing all seizures (gelastic, partial, and generalized) >30%. In Table 3, both adjusted and nonadjusted comparisons between the RS and CS groups show a positive difference in percentage seizure improvement scores: 33.54% ($P = 0.002$) and 36.02% ($P = 0.0006$), respectively.

There was a 45% increase in Engel I classification outcomes (free from disabling seizures) in the RS versus CS groups ($P = 0.001$). Conversely, there was a 40% reduction in poor outcomes (Engel class IV: no worthwhile improvement) in RS versus CS ($P = 0.0003$; Table 4). In the CS group, 33% did not respond to surgery, whereas all subjects improved in the RS group ($P = 0.0013$).

To further verify that the current study's method is an improvement over non–rs-fMRI-guided surgery, the outcomes were compared to all prior studies in the literature with at least four patients, 6 months of postoperative observation, and a minimum outcome of 75% seizure freedom rate (Table 5).[5,17,20–22] The improvement in Engel class I outcomes present in the current study is 92% versus 76%-81% in the prior studies.

TABLE 2 Percentage HH volume ablated

	C, n = 15	RS, n = 36	Total, N = 51	*P*
Total HH volume ablated				
Mean (SD)	50% (0.2)	40% (0.3)	40% (0.2)	0.1366[a]
EZ ablated				
n	0	36		
Mean (SD)		90% (10)		

C, controls; EZ, epileptogenic zone; HH, hypothalamic hamartoma; RS, resting state group; SD, standard deviation.
[a]Wilcoxon rank-sum.

3.7 | Surgical morbidity

There were no surgical side effects in either group, as assessed by a treating neurologist's examination, endocrinological testing, and postoperative neuropsychiatric assessment. In comparison with the total participants in this study (both RS and CS groups), all prior surgical reports had equal or higher permanent surgical morbidity.[5,17,20–22]

3.8 | Negative connectivity

Negative connectivity localized over venous structures was interpreted as noise. This pattern is seen best on the sagittal images of nine RS patients (Figure S3, Subjects 8, 13, 17, 18, 21, 22, 27, 28, and 32). In this study, two RS patients had predominantly negative connectivity observed from the HH to the cortex (Subjects 25 and 36, Figure S3); this was deemed likely to be significant and contributed to surgical planning.

4 | SIGNIFICANCE

This is the first time that subcentimeter rs-fMRI–identified EZs have been shown in a group study to inform epilepsy surgery with improved outcomes. Overall, the current study had the highest Engel class I outcome compared to all prior published studies.[5,17,20–22]

However, two previous studies have demonstrated better Engel class Ia, 66%-71% versus 40%.[21,22] The surgical goal of both studies was to sever the border zone between the HH and the rest of the brain. Although this technique has higher Engel class Ia outcomes, the tradeoff was greater permanent side effects, as high as 19%. This was possibly due to destruction of critical structures in and near the border zone of the HH such as the hypothalamus, mammillary bodies, fornix, mammillothalamic tract, or internal capsule.

The current technique identified an EZ regardless of its location within the HH, because every HH voxel was queried. Therefore, EZs were not limited to areas of a priori hypotheses, such as the border zone. The study's results lead to a hypothesis that the border zone could either be a conduit of epileptiform activity from an EZ located deeper in the HH, or possibly contain a primary seizure generator. Thus, unless the EZ was shown to lie within the actual border zone, it was not necessary to consider surgical intervention in this risky area.

Our data support the hypothesis that destruction of EZ improves outcomes on both ends of the Engel spectrum—higher seizure freedom/control rates (100% improved with

TABLE 3 Seizure improvement

Percentage seizure improvement	Group means, % (SD)		Difference, % (SD)	95% CI	*P*
	C	RS			
Unadjusted (raw) means	51.03 (8.66)	84.58 (5.59)	33.54 (10.31)	12.83-54.26	0.0021
Adjusted means	49.28 (8.16)	85.30 (5.25)	36.02 (9.72)	16.46-55.57	0.0006

C, controls; CI, confidence interval; RS, resting state group; SD, standard deviation.

TABLE 4 Postoperative seizure outcomes

	C, n = 15	RS, n = 36	Total, n = 51	*P*
Engel classification				0.0002[a]
Ia	6 (40.0%)	20 (55.6%)	26 (51.0%)	
Ib	1 (6.7%)	13 (36.1%)	14 (27.5%)	
III	2 (13.3%)	3 (8.3%)	5 (9.8%)	
IV	6 (40.0%)	0 (0.0%)	6 (11.8%)	
Engel I, a+b	7 (46.7%)	33 (91.7%)	40 (78.4%)	0.0010[a]
Engel Ia	6 (40%)	20 (55.6%)	26 (50.9%)	0.3678[a]
Engel III	2 (13.3%)	3 (8.3%)	5 (9.8%)	0.6239[a]
Engel IV	6 (40.0%)	0 (0.0%)	6 (11.8%)	0.0003[a]

C, controls; RS, resting state group.
[a]Fisher's exact.

TABLE 5 Review of published larger outcome reports with targeted approaches by procedure

Study	>6 Months after surgery, procedures, n	No or no worthwhile improvement, %	50% Improvement, %	75% Improvement, %	Engel class Ib, no disabling seizures, %	Engel class Ia, seizure-free, %	Total Engel class Ia and Ib, %
Wilfong & Curry 2013[5]	11	9	9	NA	36	45	81
Du et al 2017[20]	8	13		13	63	13	76
Sonoda et al 2017[21]	140	32[a]				71	79
Xu et al 2018[22]	21	29	5	NA		66	66
Current study	15 C	40	13	NA	7	40	47
	36 RS	0	8	NA	36	56	92

C, controls; NA, not appropriate; RS, resting state group.
[a]Outcomes not were reported in those who did not achieve gelastic or other seizure type freedom, except that 32% went on to have repeat surgeries.

surgery) in Engel class I and IV—with reduced surgical side effects.[21,22] This indicates that a sufficient portion of the tissue responsible for seizures was either directly or indirectly ablated by disconnecting the proximal connecting tissue to the seizure network, without destroying critical structures leading to permanent morbidity. This is especially important when destruction of the entire HH is not feasible or carries increased risk.

In 31 of 36 patients, the HH was either larger than the laser's thermal reach or irregularly shaped. In these, the rs-fMRI findings had the greatest effect on the planned laser trajectory. However, for HHs within the laser's effect size, the EZ location altered the neurosurgeon's risk/benefit analysis of targeting closer to the mammillary body or fornix than would have otherwise been approached in some cases (D.J.C.). The proximity of the rs-fMRI EZ to these structures provided information useful in determining whether not to ablate a portion of the target or to proceed with a riskier ablation, depending on the clinical details. Furthermore, even for those HHs considered "small and straightforward," the rs-fMRI mapping gave an objective measure that the EZ was within the HH, rather than at an outside location of secondary epileptogenesis. This is especially important in patients with previous HH surgery who are still experiencing seizures.

The practical aspects of this relatively new test and analysis method are important in consideration of its clinical applicability at other institutions. rs-fMRI itself is obtainable in any individual who is safe for conscious sedation in a standard MRI machine. The test adds

approximately 20 minutes to a standard MRI, thus not appreciably increasing risk of anesthesia time, nor exorbitantly increasing need for MRI scanner resources. Currently, the previously automated ICA filter step takes approximately 30 minutes of processing time and 30 minutes of analyst interpretation. The second step, SearchLight, requires 0.5-6 hours of computational processing, depending on HH size (ie, number of voxels to evaluate). The analyst's time using the SearchLight automation is reduced on average from 10 hours (which was previously a manual process) to 1 hour, with the reported range in size of HH in this study (V.L.B.). The subjectivity of the analyst's interpretations is further considered under the Limitations section below.

Applicability of this technique to other types of epilepsy may be a consideration. To support this notion, the first analysis step applied has already been shown to accurately locate EZ (although greater than subcentimeter) and improve surgical outcomes in a broad, intractable epilepsy population.[3] If this EZ is an adequate location for targeting and leads to improved surgical outcomes in both cryptogenic and symptomatic epilepsies, then it is reasonable to consider that further parsing this ICA-derived EZ by SearchLight may lead to similar improvements in seizure and morbidity outcomes, as in the current study.

The patients whose rs-fMRI was either not obtained or inadequate became control subjects. There were no perceived intrinsic differences between the control and RS group, as evidenced by no differences in Table 1. Yet, the lack of true randomization categorizes this study as level III evidence.[36] Thus, more rigorous testing is indicated to increase confidence in the findings.

4.1 | Limitations

A subjective component of image interpretation remains in this analysis paradigm. A trained expert must grade images both to categorize signal as noise versus the signals of interest and to determine the presence or absence of rs-fMRI connectivity of the HH with the rest of the brain. Thus, this method is prone to the same subjectivities and biases as nearly all clinically determined radiographic images, highlighting an area of potential technique improvement.[37–39]

Understanding normal resting state connectivity between the hypothalamus and the rest of the brain may also help distinguish pathological from nonpathological signals. The current basis of our interpretation of abnormal functional connectivity from the HH is that any connectivity from the hamartoma to elsewhere in the brain is abnormal, presuming no normal connectivity from the HH. Although the center of the brain contains a denser vascularity, which increases the potential total contribution to the blood oxygenation level–dependent signal not related to neural-vascular coupling,[40] ICA denoising of these influences leads to improved seizure outcomes. However, our postoperative rs-fMRIs in seizure-free patients are not fully analyzed to help make this determination. Conversely, the hypothalamus, which is a different structure from the HH, does have a typical connectivity signature in normal adults to the thalamus, ventromedial prefrontal cortex, and other areas.[41,42] The normal connectivity of the hypothalamus was not systematically queried as part of this study. Unfortunately, there are currently no normal pediatric hypothalamic connectivity studies. Furthermore, children with intractable epilepsy from HH would likely be poor candidates to help determine normal hypothalamic connectivity. Normal controls without an HH were not included to make this determination because of IRB or ethical concerns. One avenue for elucidating what is possible to detect with resting state fMRI may be to collect data at much higher resolution at greater field strength (eg, 7 T). This will assist interpretations of our technique and findings in relation to what is possible to observe using noninvasive human neuroimaging.

It is known that seizures come from within the HH[3–5] and cannot be further localized by MRI-based anatomical attributes. rs-fMRI locates where the HH is functionally connected to the rest of the brain. These internal HH locations are candidates for seizure spread. The term rs-fMRI EZ was used to denote the IC showing connectivity between the HH and elsewhere in the brain by visible inspection. The primary proof that the rs-fMRI EZ was truly involved in seizure generation is the improved outcomes of the RS group. An indirect validation was the connectivity pattern to the same areas in prior studies with other methodologies,[16] and this may serve as one preliminary validation when future replication studies are considered. Otherwise, there was no outside, direct validation technique, such as depth electrode verification. Notably, the shape and location of RS targets were highly variable (as seen in Figure S3). Thus, individual rs-fMRI is required to inform surgery, and not generalizable to other surgical approaches.

Another limitation is that the voxel size of the acquired resting state scan was $3.0 \times 3.0 \times 3.4$ mm, or 30.6 mm^3. The RS subjects' HH ranged in size from 0.9 to 28.3 cm^3, with a mean of 8.1 cm^3. Thus, we cannot exclude the possibility of a higher partial volume averaging effect for the small HHs. Decreasing voxel size may reduce partial volume effects and susceptibility artifacts,[43] with the primary tradeoff being significantly increased scanner and sedation times (traditionally nearly two or three times the time for a 30% decrease in voxel volume). New fMRI sequence optimization methodologies, however, hold promise to mitigate this issue.[44]

Lastly, the surgeon did not create a map of where the surgical target would have been without rs-fMRI guidance. It is possible that some or all of the rs-fMRI target was randomly included. Evidence that speaks against that is the surgeon's description of approach in RS versus CS groups in the Materials and Methods and Significance sections, but also the quantified amount of rs-fMRI target ablated. Namely, the RS and CS groups had 40% and 50%, respectively, ablated of the total HH, yet the rs-fMRI target ablation percentage was substantially higher at 87.5%. Conversely, it would be reasonable to expect only 40%-50% rs-fMRI target ablation if the surgeon were taking the same approach in both groups. Furthermore, with a 45% reduction in the RS group compared to controls, it seems unlikely that this was due to chance alone.

4.2 | Future directions

The effort to study intraoperative rs-fMRI target guidance for epilepsy is underway. Ideally, rs-fMRI can be repeated after the initial lasering, similar to that reported in Boerwinkle et al,[45] querying connectivity to determine whether the rs-fMRI target was ablated and to what extent further lesion creation is necessary to adequately disconnect the EZ from propagation pathways. Repeat ablation may be necessary during the same operative period, with repeated rs-fMRI scanning and rapid analyses to check for adequate disconnection. This may improve surgical outcomes and reduce the need for repeat surgeries. Equally of interest is the potential to use resting state fMRI to guide interoperative safety markers. For example, the mammillary bodies are immediately proximal to the HH and are critical in establishing new memories. Ensuring the continued typical pattern of connectivity from the HH to the anterior thalamus could also be checked during such an iterative procedure.

Investigators may compare their patient's rs-fMRI results directly to the entire subject image dataset in Figure S3 to aid with interpretation. The endeavor to crystalize the HH epileptogenic network may parse subsets of HH epileptogenic network patterns. Furthermore, it may become better understood if these patterns correlate with different subcategories of seizure semiology and clinical course.

Epilepsy in children with HH is associated with encephalopathy.[4] The encephalopathy is thought to be reduced in children when effective surgery is performed earlier in life.[21,46–55] However, some children continue to have behavioral and neurodevelopmental concerns, despite substantial seizure reduction. rs-fMRI may enable localization of a putative disrupted network pattern if the investigator compares those patterns with the patterns of patients who experience postoperative normalized development. Such localization of neurodevelopmentally based disorder may inform future therapies with location-targeted strategies.

5 | CONCLUSION

This is the first time rs-fMRI localized subcentimeter-sized targets have been used to prospectively guide surgical planning. This approach is shown to be technically feasible and can significantly improve freedom from disabling seizures in intractable epilepsy. Our technique improved freedom from seizures by 45% and reduced outcomes with no worthwhile improvement in seizure control by 40% compared to conventional ablation, regardless of hamartoma size or anatomical classification. The rs-fMRI voxelwise/subcentimeter-based targeting for SLA for HH, termed SearchLight, may be considered for precise and effective ablation. This approach may in turn be applicable to all those with intractable focal epilepsies.

ACKNOWLEDGMENTS

In loving memory of Grace Katherine Webster, who inspired the effort to propel forward the technology to improve and cure the epilepsy of other children the world over with hypothalamic hamartoma.

DISCLOSURE

The authors have no conflicts of interest to report. We confirm that we have read the Journal's position on issues involved in ethical publication and affirm that this report is consistent with those guidelines.

ORCID

Varina L. Boerwinkle http://orcid.org/0000-0002-1429-2994

REFERENCES

1. Chen Z, Brodie MJ, Liew D, Kwan P. Treatment outcomes in patients with newly diagnosed epilepsy treated with established and new antiepileptic drugs: a 30-year longitudinal cohort study. JAMA Neurol. 2018;75:279–86.
2. Luders HO, Najm I, Nair D, Widdess-Walsh P, Bingman W. The epileptogenic zone: general principles. Epileptic Disord. 2006;8 (suppl 2):S1–9.
3. Boerwinkle VL, Mohanty D, Foldes ST, et al. Correlating resting-state functional magnetic resonance imaging connectivity by independent component analysis-based epileptogenic zones with intracranial electroencephalogram localized seizure onset zones and surgical outcomes in prospective pediatric intractable epilepsy study. Brain Connect. 2017;7:424–42.
4. Kerrigan JF, Ng YT, Chung S, Rekate HL. The hypothalamic hamartoma: a model of subcortical epileptogenesis and encephalopathy. Semin Pediatr Neurol. 2005;12:119–31.

5. Wilfong AA, Curry DJ. Hypothalamic hamartomas: optimal approach to clinical evaluation and diagnosis. Epilepsia. 2013;54 (suppl 9):109–14.
6. Kerrigan JF, Parsons A, Tsang C, Simeone K, Coons S, Wu J. Hypothalamic hamartoma: neuropathology and epileptogenesis. Epilepsia. 2017;58(suppl 2):22–31.
7. Steinmetz PN, Wait SD, Lekovic GP, Rekate HL, Kerrigan JF. Firing behavior and network activity of single neurons in human epileptic hypothalamic hamartoma. Front Neurol. 2013;4:210.
8. Wu J, Gao M, Shen JX, Qiu SF, Kerrigan JF. Mechanisms of intrinsic epileptogenesis in human gelastic seizures with hypothalamic hamartoma. CNS Neurosci Ther. 2015;21:104–11.
9. Baroncini M, Jissendi P, Balland E, et al. MRI atlas of the human hypothalamus. Neuroimage. 2012;59:168–80.
10. Lauterbach EC, Cummings JL, Kuppuswamy PS. Toward a more precise, clinically–informed pathophysiology of pathological laughing and crying. Neurosci Biobehav Rev. 2013;37:1893–916.
11. Kokkinos V, Zountsas B, Kontogiannis K, Garganis K. Epileptogenic networks in two patients with hypothalamic hamartoma. Brain Topogr. 2012;25:327–31.
12. Kuzniecky R, Guthrie B, Mountz J, et al. Intrinsic epileptogenesis of hypothalamic hamartomas in gelastic epilepsy. Ann Neurol. 1997;42:60–7.
13. Leal AJ, Monteiro JP, Secca MF, Jordão C. Functional brain mapping of ictal activity in gelastic epilepsy associated with hypothalamic hamartoma: a case report. Epilepsia. 2009;50:1624–31.
14. Nguyen D, Singh S, Zaatreh M, et al. Hypothalamic hamartomas: seven cases and review of the literature. Epilepsy Behav. 2003;4: 246–58.
15. Fox MD, Raichle ME. Spontaneous fluctuations in brain activity observed with functional magnetic resonance imaging. Nat Rev Neurosci. 2007;8:700–11.
16. Boerwinkle VL, Wilfong AA, Curry DJ. Resting-state functional connectivity by independent component analysis-based markers corresponds to areas of initial seizure propagation established by prior modalities from the hypothalamus. Brain Connect. 2016;6:642–51.
17. Regis J, Helen Cross J, Kerrigan JF. Achieving a cure for hypothalamic hamartomas: a Sisyphean quest? Epilepsia. 2017;58 (suppl 2):7–11.
18. Sommer B, Schlaffer SM, Coras R, et al. Intraoperative use of high-field MRI in hypothalamic hamartomas associated with epilepsy: clinico-pathological presentation of five adult patients. Acta Neurochir (Wien). 2014;156:1865–78.
19. Drees C, Chapman K, Prenger E, et al. Seizure outcome and complications following hypothalamic hamartoma treatment in adults: endoscopic, open, and Gamma Knife procedures. J Neurosurg. 2012;117:255–61.
20. Du VX, Gandhi SV, Rekate HL, Mehta AD. Laser interstitial thermal therapy: a first line treatment for seizures due to hypothalamic hamartoma? Epilepsia. 2017;58(suppl 2):77–84.
21. Sonoda M, Masuda H, Shirozu H, et al. Predictors of cognitive function in patients with hypothalamic hamartoma following stereotactic radiofrequency thermocoagulation surgery. Epilepsia. 2017;58:1556–65.
22. Xu DS, Chen T, Hlubek RJ, et al. Magnetic resonance imaging-guided laser interstitial thermal therapy for the treatment of hypothalamic hamartomas: a retrospective review. Neurosurgery. 2018 Jan 13 [Epub ahead of print].
23. Delalande O, Fohlen M. Disconnecting surgical treatment of hypothalamic hamartoma in children and adults with refractory epilepsy and proposal of a new classification. Neurol Med Chir (Tokyo). 2003;43:61–8.
24. Zubkov S, Del Bene VA, MacAllister WS, Shepherd TM, Devinsky O. Disabling amnestic syndrome following stereotactic laser ablation of a hypothalamic hamartoma in a patient with a prior temporal lobectomy. Epilepsy Behav Case Rep. 2015;4:60–2.
25. Lee HW, Arora J, Papademetris X, et al. Altered functional connectivity in seizure onset zones revealed by fMRI intrinsic connectivity. Neurology. 2014;83:2269–77.
26. Zhang CH, Lu Y, Brinkmann B, Welker K, Worrell G, He B. Lateralization and localization of epilepsy related hemodynamic foci using presurgical fMRI. Clin Neurophysiol. 2015;126:27–38.
27. Jackson GD, Pedersen M, Harvey AS. How small can the epileptogenic region be? A case in point. Neurology. 2017;88:2017–9.
28. Engel J Jr. Update on surgical treatment of the epilepsies. Summary of the Second International Palm Desert Conference on the Surgical Treatment of the Epilepsies (1992). Neurology. 1993;43:1612–7.
29. Beckmann CF, Smith SM. Probabilistic independent component analysis for functional magnetic resonance imaging. IEEE Trans Med Imaging. 2004;23:137–52.
30. Griffanti L, Douaud G, Bijsterbosch J, et al. Hand classification of fMRI ICA noise components. Neuroimage. 2017;154:188–205.
31. Greicius MD, Supekar K, Menon V, Dougherty RF. Resting-state functional connectivity reflects structural connectivity in the default mode network. Cereb Cortex. 2009;19:72–8.
32. Honey CJ, Sporns O, Cammoun L, et al. Predicting human resting-state functional connectivity from structural connectivity. Proc Natl Acad Sci U S A. 2009;106:2035–40.
33. Beckmann CF, Smith SM. Tensorial extensions of independent component analysis for multisubject FMRI analysis. Neuroimage. 2005;25:294–311.
34. Cox RW. AFNI: software for analysis and visualization of functional magnetic resonance neuroimages. Comput Biomed Res. 1996;29:162–73.
35. Fox MD, Greicius M. Clinical applications of resting state functional connectivity. Front Syst Neurosci. 2010;4:19.
36. Sackett DL, Rosenberg WM, Gray JA, Haynes RB, Richardson WS. Evidence based medicine: what it is and what it isn't. BMJ. 1996;312:71–2.
37. Jeurissen B, Descoteaux M, Mori S, Leemans A. Diffusion MRI fiber tractography of the brain. NMR Biomed. 2017 Sep 2 [Epub ahead of print].
38. McCarthy AL, Winters ME, Busch DR, et al. Scoring system for periventricular leukomalacia in infants with congenital heart disease. Pediatr Res. 2015;78:304–9.
39. Zafar SF, Westover MB, Gaspard N, et al. Interrater agreement for consensus definitions of delayed ischemic events after aneurysmal subarachnoid hemorrhage. J Clin Neurophysiol. 2016;33:235–40.
40. Buxton RB, Uludag K, Dubowitz DJ, Liu TT. Modeling the hemodynamic response to brain activation. Neuroimage. 2004;23 (suppl 1):S220–33.
41. Sudheimer K, Keller J, Gomez R, et al. Decreased hypothalamic functional connectivity with subgenual cortex in psychotic major depression. Neuropsychopharmacology. 2015;40:849–60.
42. Kaufmann C, Wehrle R, Wetter TC, et al. Brain activation and hypothalamic functional connectivity during human non-rapid eye movement sleep: an EEG/fMRI study. Brain. 2006;129:655–67.

43. Iranpour J, Morrot G, Claise B, Jean B, Bonny JM. Using high spatial resolution to improve BOLD fMRI detection at 3T. PLoS One. 2015;10:e0141358.
44. Chen L, T Vu A, Xu J, et al. Evaluation of highly accelerated simultaneous multi-slice EPI for fMRI. Neuroimage. 2015;104: 452–9.
45. Boerwinkle VL, Vedantam A, Lam S, Wilfong AA, Curry DJ. Connectivity changes after laser ablation: resting-state fMRI. Epilepsy Res. 2017;142:156–60.
46. Addas B, Sherman EM, Hader WJ. Surgical management of hypothalamic hamartomas in patients with gelastic epilepsy. Neurosurg Focus. 2008;25:E8.
47. Chibbaro S, Cebula H, Scholly J, et al. Pure endoscopic management of epileptogenic hypothalamic hamartomas. Neurosurg Rev. 2017;40:647–53.
48. Khawaja AM, Pati S, Ng YT. Management of epilepsy due to hypothalamic hamartomas. Pediatr Neurol. 2017;75:29–42.
49. Mittal S, Mittal M, Montes JL, Farmer JP, Andermann F. Hypothalamic hamartomas. Part 2. Surgical considerations and outcome. Neurosurg Focus. 2013;34:E7.
50. Pati S, Sollman M, Fife TD, Ng YT. Diagnosis and management of epilepsy associated with hypothalamic hamartoma: an evidence-based systematic review. J Child Neurol. 2013;28:909–16.
51. Regis J, Scavarda D, Tamura M, et al. Epilepsy related to hypothalamic hamartomas: surgical management with special reference to Gamma Knife surgery. Childs Nerv Syst. 2006;22:881–95.
52. Regis J, Scavarda D, Tamura M, et al. Gamma Knife surgery for epilepsy related to hypothalamic hamartomas. Semin Pediatr Neurol. 2007;14:73–9.
53. Rosenfeld JV. The evolution of treatment for hypothalamic hamartoma: a personal odyssey. Neurosurg Focus. 2011;30:E1.
54. Schulze-Bonhage A, Trippel M, Wagner K, et al. Outcome and predictors of interstitial radiosurgery in the treatment of gelastic epilepsy. Neurology. 2008;71:277–82.
55. Wethe JV, Prigatano GP, Gray J, Chapple K, Rekate HL, Kerrigan JF. Cognitive functioning before and after surgical resection for hypothalamic hamartoma and epilepsy. Neurology. 2013;81: 1044–50.

SUPPORTING INFORMATION

Additional supporting information may be found online in the Supporting Information section at the end of the article.

How to cite this article: Boerwinkle VL, Foldes ST, Torrisi SJ, et al. Subcentimeter epilepsy surgery targets by resting state functional magnetic resonance imaging can improve outcomes in hypothalamic hamartoma. *Epilepsia*. 2018;00:1–12. https://doi.org/10.1111/epi.14583